Published in final edited form as:
Mol Cell. 2012 September 28; 47(6): 933–942. doi:10.1016/j.molcel.2012.07.001.

Structure of an E3:E2~Ub complex reveals an allosteric mechanism shared among RING/U-box ligases

Jonathan N. Pruneda[1], **Peter J. Littlefield**[1], **Sarah E. Soss**[2], **Kyle A. Nordquist**[2], **Walter J. Chazin**[2], **Peter S. Brzovic**[1], and **Rachel E. Klevit**[1,§]

[1]Department of Biochemistry, University of Washington, Seattle, Washington 98195, United States

[2]Department of Biochemistry, Vanderbilt University, Nashville, Tennessee 37232, United States

Abstract

Despite the widespread importance of RING/U-box E3 ubiquitin ligases in ubiquitin (Ub) signaling, the mechanism by which this class of enzymes facilitates Ub transfer remains enigmatic. Here we present a structural model for a RING/U-box E3:E2~Ub complex poised for Ub transfer. The model and additional analyses reveal that E3 binding biases dynamic E2~Ub ensembles toward closed conformations with enhanced reactivity for substrate lysines. We identify a key hydrogen bond between a highly conserved E3 sidechain and an E2 backbone carbonyl, observed in all structures of active RING/U-Box E3/E2 pairs, as the linchpin for allosteric activation of E2~Ub. The conformational biasing mechanism is generalizable across diverse E2s and RING/U-box E3s, but is not shared by HECT-type E3s. The results provide a structural model for a RING/U-box E3:E2~Ub ligase complex and identify the long sought-after source of allostery for RING/U-Box activation of E2~Ub conjugates.

Introduction

Post-translational protein modification by ubiquitin (Ub) is critical for control of a broad range of cellular pathways. Yet mechanistic details of Ub transfer are poorly understood. The basic scheme of Ub activation and transfer requires the sequential activity of three enzymes; an E1 Ub-activating enzyme, an E2 Ub-conjugating enzyme, and an E3 Ub-ligase. There are two predominant classes of E3s: 1) HECT ligases, which act via obligate formation of an E3~Ub thioester intermediate, and 2) RING/U-box ligases, which facilitate the direct transfer of Ub from an E2~Ub conjugate to a target substrate. In the absence of an E3, the reactivity of E2~Ub conjugates toward small nucleophiles is significantly reduced. This behavior presumably prevents nonproductive hydrolysis of the Ub-thioester bond

[§]To whom correspondence should be addressed: University of Washington, Box 357350, Seattle, WA 98195. Telephone: (206) 543-5891. Fax: (206) 543-8394. klevit@uw.edu.

Author Contributions

J.N.P and P.J.L. performed all experiments, with the exception of NMR relaxation studies performed by S.E.S. and E4B auto-ubiquitination assays performed by K.A.N. J.N.P., P.J.L., P.S.B., and R.E.K. designed the overall study and J.N.P., P.J.L., P.S.B., W. J. C., and R.E.K. analyzed the data and wrote the manuscript.

The authors declare no competing financial interests. DNA constructs will be made available through Addgene.org. Coordinates for the HADDOCK ensemble of the ternary complex are available for download at http://depts.washington.edu/klvtlab/ (Protein Portraits tab).

before assembly into an E3-ligase Ub-transfer complex. Thus, RING/U-box E3 ligases not only coordinately bind E2~Ub conjugate and substrate, but must also activate the E2~Ub thioester to enhance the direct transfer of Ub to a target lysine (Song et al., 2009; Wenzel et al., 2011).

The structural basis for RING/U-box-mediated E2~Ub activation has been elusive. Numerous structural studies have allowed definition of a consensus E3:E2 contact surface comprised of E2 residues located in Helix 1, Loop 4, and Loop 7, and RING/U-box residues in Loops 1, 2, and the central Helix (Fig 1A). This arrangement places the E2 active site ~15Å away from the E3:E2 interface (Zheng et al., 2000; Benirschke et al., 2010; Yin et al., 2009; Xu et al., 2008; Deshaies et al., 2009; Zhang et al., 2005; Bentley et al., 2011). No clear structural differences between free and E3-bound E2s are apparent that explain E3 enhancement of E2~Ub reactivity. Using statistical coupling analysis, Ozkan et. al. (2005) identified clusters of co-evolving residues in UbcH5b that link the E3-binding interface to the E2 active site. Based upon mutational analysis, they suggested that RING-type E3s may allosterically activate E2s, but the structural basis for the E3-dependent activation was not defined (Ozkan et al., 2005). Here we report structural and biochemical studies that define how RING/U-box E3 ligases allosterically activate E2~Ub conjugates.

Our studies focus on interactions of UbcH5c~Ub with two RING/U-box E3s, BRCA1/BARD1 (Welcsh et al., 2000; Welcsh et al., 2001; Yu, 2000; Scully et al., 2002) and E4B (Cyr et al., 2002; Richly et al., 2005). The UbcH5 family of E2 Ub-conjugating enzymes are among the most thoroughly characterized, both structurally and biochemically, including interactions between unconjugated UbcH5 and BRCA1/BARD (Brzovic et al., 2003; Christensen et al., 2007) and E4B (Benirschke et al., 2010; Nordquist et al., 2010). Analysis of the UbcH5c~Ub conjugate in the absence of an E3 revealed it to be highly dynamic. UbcH5c~Ub displays a preference for highly extended and open conformations (few non-covalent interactions between E2 and Ub domains) and only occasionally samples closed conformations in which the Ub subunit directly contacts Helix 2 of the E2 (Fig 1B) (Pruneda et al., 2011). Closed E2~Ub conformations were first proposed for Ub conjugated to the yeast E2 Ubc1, and recent studies have linked closed E2~Ub conformational states to the ability of the E2s Ube2s and Cdc34 to transfer Ub in E3-*independent* reactions (Hamilton et al., 2001; Wickliffe et al., 2011; Saha et al., 2011). While it might seem logical to extend these observations to infer that E3 binding is associated with closed E2~Ub, states, there is no experimental evidence that directly addresses this point.

Here, we present an experimentally-based structural model for an E3:E2~Ub ternary complex. We show that binding of either BRCA1/BARD1 or E4B promotes a shift in the dynamic ensemble of UbcH5c~Ub, biasing the conjugate toward closed conformations that are more reactive for Ub transfer. Structural analysis of an E3:E2~Ub complex allowed us to design targeted mutations that selectively disrupt E3-enhanced Ub transfer without affecting consensus E3:E2 interactions, thereby uncoupling E3 binding from activation. We identify a highly conserved E3 sequence motif and an essential E3:E2 hydrogen bond that serves as the linchpin for activation of E2~Ub conjugates. This work supports a model in which RING/U-box E3 ligases allosterically activate E2~Ub conjugates for transfer through a broadly conserved mechanism.

Results

Interactions of protein subunits within the E4BU:UbcH5c~Ub ligase complex

Assembly of a RING or U-box E3:E2~Ub complex poised for Ub transfer involves simultaneous interactions among multiple components. The interactions are of moderate to weak affinity, resulting in the formation of a dynamic E3:E2~Ub structural ensemble. To

generate a structural model of the E4B:UbcH5c~Ub complex we used NMR chemical shift perturbations (CSPs) and paramagnetic relaxation probes to characterize interactions among the various protein subunits. NMR experiments for structural analysis were performed with the E4B minimal U-Box construct (E4BU; residues 1092–1173) and UbcH5c (free and Ub-conjugated) with a Cys85Ser mutation to produce a more stable oxyester-linked UbcH5c-O~Ub conjugate (Brzovic et al., 2006). Separate isotopic labeling of E4BU, UbcH5c, and Ub subunits allowed for the identification of each protein-protein interaction surface within the ternary complex using $^{1}H,^{15}N$-HSQC-TROSY NMR titration experiments (Fig S1). Criteria used for determining contact residues included solvent accessibility and chemical shift perturbations greater than one standard deviation above the mean. Results from NMR titration experiments were used to generate sets of ambiguous interaction restraints (AIRs), which in turn were used for the structure calculations and docking in HADDOCK (de Vries et al., 2010). A complete list of restraints is provided in Table S1. For the E4BU:UbcH5~Ub complex, 200 structures were calculated and the top-scoring cluster was selected. This cluster contained 36 structures with an average pairwise RMSD of 2.87Å (Fig 1C).

Chemical shift perturbations (CSPs) similar in trajectory and magnitude (Fig S1A, S1B, S1H) are observed for residues comprising the consensus E3:E2 contact surface for E4BU binding to both free UbcH5c and UbcH5c~Ub. These data indicate that the consensus contact surface between E4BU and UbcH5c is maintained whether or not conjugated Ub is present (Fig 1A, 1C). Consistent with this observation, comparison of the E4BU and UbcH5c subunits in the NMR-based ensemble to an E4BU:UbcH5c co-crystal structure yields an average pairwise RMSD of 1.68Å over all members of the cluster (Benirschke et al., 2010).

Additional CSPs outside the consensus E3:E2 interaction site are observed in both the UbcH5c and Ub subunits upon formation of the E4BU:UbcH5c~Ub ternary complex (Fig S1A, S1C). In UbcH5c, the additional CSPs observed are for residues in Helix 2 (centered around Leu104) and surrounding the E2 active site (residues His75, Asn77, and Leu86) (Fig S1B). The CSPs in Ub map to a region centered about Leu8, Ile44, and V70, which form a surface exposed hydrophobic patch utilized in many Ub-protein interactions (Fig S1D). As compared to UbcH5c~Ub in the absence of an E3, which populates mainly extended conformations (Pruneda et al., 2011), these data show that the I44 surface of the Ub subunit interacts more frequently with solvent exposed residues centered around Leu 104 in Helix 2 of UbcH5c while in the ternary complex. These CSPs for resonances in the regions of UbcH5c and Ub serve as signatures for adjustments in the UbcH5c~Ub ensemble toward closed conformations. Similar observations were made in NMR titrations performed with the BRCA1/BARD1 RING heterodimer reveal that RING E3 interactions also shift UbcH5c~Ub conformations toward more closed conformational states (Fig S1I).

Within the structural ensemble of the ternary complex, the relative position of Ub displays the largest variability. In individual members of the ensemble, the potential E4BU:Ub interface varies from essentially no contact to almost 300$Å^2$. Within the ensemble, residues in Ub β-strand 2 approach residues in C-terminal region of E4BU Loop 2. The interaction between Ub and UbcH5c is more defined and extensive, comprised of a combination of hydrophobic and electrostatic interactions. The most prominent of the electrostatic contacts are between a negatively-charged patch on UbcH5c comprised of Asp42, Asp112, Asp116, Asp117 and a positively-charged patch on Ub formed by Arg42, Lys48, and Arg72 (Fig 1D).

TEMPO spin labels incorporated into various positions of Ub provide independent verification of the ternary complex calculated from CSPs. NMR spectra were collected to identify UbcH5c and E4BU residues affected by proximity to a paramagnetic probe in the

E3:E2~Ub complex. Ub-K11SL affected many of the same residues in UbcH5c reported previously for the conjugate alone (Pruneda et al., 2011) (i.e. Loop 1 and Helix 2), but the effects in Loop 7 are of significantly greater magnitude in the ternary complex (Fig 1E, S1J). Ub-K11SL also affected E4BU residues in Loop 1, the β1/β2 turn, Helix 1, and Loop 2 (Fig 1E, S1K). Together, the paramagnetic spin label data confirm both the interacting surfaces and the orientation of subunits in the structural model of the complex derived from CSPs.

NMR heteronuclear relaxation measurements were performed to ascertain whether the closed conformations of UbcH5~Ub observed in the structural ensemble of the ternary complex are associated with a change in the dynamics of the E2~Ub conjugate. The relaxation parameters were used to define diffusion tensors that describe the overall tumbling for Ub in the isolated UbcH5c~Ub conjugate and within the E4BU:UbcH5c~Ub ternary complex (Palmer, 2004). Figure 1F shows a mesh representation of the diffusion tensor of ubiquitin in the UbcH5c conjugate alone and in complex with E4BU. There is a 16% reduction in the volume of the tensor calculated for the E4BU complex compared to the UbcH5c~Ub conjugate alone (Fig 1F, Table S2). This analysis demonstrates that the motion of the conjugated Ub is significantly slowed upon E4BU binding to the conjugate.

E2~Ub closed conformations are necessary for E3-mediated Ub transfer

The E4BU:UbcH5c~Ub structural ensemble predicts contact residues that should be important for stabilizing the complex in closed conformations. Point mutations in UbcH5c and in Ub were generated to test these predictions (Fig 2A). UbcH5c Leu104 is a solvent exposed hydrophobic residue on Helix 2 for which significant CSPs are observed upon formation of the E4BU:UbcH5c-O~Ub complex. The structurally analogous position is widely conserved as a hydrophobic residue among E2s that function with RING/U-box E3s (Fig S2A). Hence, Leu104 was mutated to glutamine to disrupt hydrophobic non-covalent interactions between UbcH5c and Ub. For Ub, each residue of the Leu8-Ile44-Val70 hydrophobic surface was mutated to Ala. Titration of unlabeled E4BU into ^{15}N-UbcH5c^{L104Q}-O~^{15}N-Ub or ^{15}N-UbcH5c-O~^{15}N-Ub^{I44A} produced CSPs nearly identical to those observed for free UbcH5c (Fig S1, S3). Notably, CSP signatures for UbcH5c~Ub closed conformational states were not observed, even though the designed point mutations do not appear to affect consensus E3:E2 interactions. From the perspective of the E3, titration of ^{15}N-E4BU with either UbcH5c-O~Ub^{I44A} or UbcH5c^{L104Q}-O~Ub resulted in CSPs in E4BU nearly identical to those observed for interactions between E4BU and free UbcH5c (Fig S1E, S1G). Thus, the designed mutations in Ub and UbcH5c uncouple the E3-induced conformational shift in the UbcH5c~Ub ensemble from consensus E3:E2 binding and can, therefore, be used to assess the functional role of closed conformational states in E3-mediated Ub transfer reactions.

The impact of the designed mutations on Ub transfer reactions were examined using auto-ubiquitination assays in which the E3 serves as both ligase and proxy substrate. The BC$_{304}$/BD$_{327}$ heterodimer (BRCA1 residues 1–304, BARD1 residues 26–327) and E4BU^{+20} (E4BU with an additional 20 N-terminal residues) were used in activity assays as these longer constructs are more efficient proxy substrates than the minimal RING or U-box domains used in NMR experiments (Christensen et al., 2007; Nordquist et al., 2010). In these experiments, no auto-ubiquitination of either BC$_{304}$/BD$_{327}$ or E4BU^{+20} was observed in reactions involving UbcH5c^{L104Q}, Ub^{L8A}, Ub^{I44A}, or Ub^{V70A} (Fig 2B, S4A, S4B). More conservative substitutions, UbcH5c^{L104V} and Ub^{V70I}, display intermediate levels of Ub transfer activity (Fig S4A, S4B). None of the UbcH5c and Ub mutations affected charging of Ub onto the E2. Thus, inclusion of mutant versions of either component (E2 or Ub) severely diminishes or abrogates Ub transfer activity and the differences in activity reflect changes in the final step of Ub transfer from the E2 onto a substrate lysine.

Reaction of the UbcH5c~Ub thioester with the ε-amino group of free lysine provides a direct measure for the intrinsic aminolysis activity of an E2~Ub conjugate in the absence and presence of a RING/U-box E3 (Wenzel et al., 2011). The ability of UbcH5c~Ub to transfer Ub to free lysine was monitored in the presence of BC_{112}/BD_{140} (BRCA1 residues 1–112, BARD1 residues 26–140). Compared to a $BRCA1^{I26A}$ control that abrogates UbcH5c binding (Brzovic et al., 2003), the reactivity of the UbcH5c~Ub conjugate toward lysine is dramatically increased by the presence of BC_{112}/BD_{140}, indicating an E3-induced activation of the UbcH5c~Ub thioester to nucleophilic attack (Wenzel et al., 2011). Mutant E2~Ub conjugates comprised of either $UbcH5c^{L104Q}$ or Ub^{I44A} are marginally slower in E3-independent aminolysis assays, consistent with previous reports (Wickliffe et al., 2011; Saha et al., 2011). Importantly, no enhancement of reactivity is observed upon addition of BC_{112}/BD_{140}, despite the ability of the mutant UbcH5c~Ub conjugates to bind the E3 (Fig 2C). Therefore, the consensus E2:E3 interaction is necessary but not sufficient to enhance UbcH5c~Ub reactivity.

Though the UbcH5c-O~Ub conjugate used in our NMR experiments is more stable toward hydrolysis than the thioester conjugate, the oxyester-linked conjugate undergoes enhanced hydrolysis in the presence of stoichiometric amounts of E4BU. As a quantitative measure of the E3 rate enhancement, UbcH5c-O~Ub hydrolysis was monitored by 1D-NMR. The Asn77 backbone amide resonance undergoes a well-resolved chemical shift change upon formation of the UbcH5c-O~Ub conjugate and serves as an indicator of the relative amounts of E2~Ub and free E2 present. 1D ^{1}H spectra were collected at twenty-minute intervals after addition of E4BU and the area of the conjugated-Asn77 resonance was plotted as a function of time. In the absence of E4BU, the UbcH5c-O~Ub oxyester hydrolyzed slowly, with a half-life of approximately 58 hours at 25°C. Addition of an equimolar amount of E4BU decreased the oxyester half-life to less than 10 hours. The E3-mediated rate enhancement (i.e., $k_{obs}(E3)/k_{obs}(no\ E3)$) corresponds to a $\Delta\Delta G^{\ddagger}$ of approximately 1 kcal/mol. Complexes formed with mutations that disfavor closed conformations (ie. $UbcH5c^{L104Q}$ or Ub^{I44A}) have rates of hydrolysis nearly identical to the no-E3 control (Fig 2D). Taken together, the activity assays reveal a strong correlation between E3-mediated Ub transfer and the induced UbcH5c~Ub closed conformations observed in NMR CSP experiments. Thus, mutations that block the ability of E3 to shift the UbcH5c~Ub ensemble toward closed conformations also block E3 enhancement of Ub transfer.

Conformational activation is a general feature of RING/U-box E3:E2~Ub function

Of the twenty human Ub-conjugating E2s with known structures, twelve have a leucine that is structurally analogous to UbcH5c Leu104, and two others have methionine at this position, suggesting the position plays a similar role in other E2s. A set of E2s that function with BRCA1/BARD1 was used to examine the generalizability of the conformational activation mechanism among E2s. The representative E2s investigated were Ube2e1 (transfers monoubiquitin), Ube2K (synthesizes K48-linked chains), and Ube2n (synthesizes K63-linked chains with Uev1A) (Christensen et al., 2007). In each E2, the mutation analogous to UbcH5c L104Q substantially decreases BRCA1/BARD1-enhanced reactivity toward lysine (Fig 3A).

To assess whether other RING/U-box E3s function via similar mechanisms to activate the UbcH5c~Ub conjugate, assays were performed using either wild-type or L104Q UbcH5c and the RING E3s MDM2 (a homodimeric C-terminal RING), RNF8 (a structurally uncharacterized N-terminal RING), and SCF-Fbw7 (a multi-component RING E3). MDM2 and RNF8 auto-ubiquitination activity is drastically decreased when UbcH5c L104Q is the E2 (Fig 3B). SCF-Fbw7-dependent ubiquitination of the substrate cyclin E was similarly affected (Fig S4C). In stark contrast, Ub transfer catalyzed by HECT-type E3 ligases (which proceeds via a transthiolation reaction to generate an E3~Ub thioester intermediate) is

unaffected by the UbcH5c L104Q mutation, as shown in assays using E6AP, SspH1 (a bacterial effector protein), and HHARI (a RBR RING/HECT hybrid) as the E3 (Fig 3C). Thus, diverse E2s and RING/U-box E3s utilize a similar mechanism whereby activation of an E2~Ub conjugate by a RING/U-box E3 ligase requires that E2~Ub closed conformations be populated. This shared mechanism implies that a conserved feature in RING/U-box E3s is responsible for the activation of E2~Ub conjugates, but to date no such feature has been identified.

Formation of a conserved E3:E2 hydrogen bond increases the population of E2~Ub closed conformations

The structural model of E4BU:UbcH5c~Ub indicates that Loop 2 of E4BU occupies conformations in which it is in intimate contact with UbcH5c. Comparison of the sequence of this loop across RING and U-box E3s revealed a highly conserved Φ-x-(K/R) motif, where Φ is a hydrophobic residue and x is either the final Cys of RING domains or a corresponding polar residue of U-box domains that is important for structural stability (for example E4B residues F1141-N1142-R1143 or BRCA1 residues L63-C64-K65) (Fig S2B). Analysis of structurally homologous E3 residues in all available high-resolution RING/U-box E3:E2 co-crystal structures (PDB IDs 1FBV, 2C2V, 2OXQ, 3HCT, 3L1Z, and 3RPG) revealed that the conserved K/R side chain forms a hydrogen bond with an E2 backbone carbonyl preceding Loop 7 (corresponding to UbcH5c residue 92) (Fig 4A, S5A). This hydrogen bond is strictly conserved among all deposited structures (in the case of TRAF6:Ubc13, the connection is made through a water molecule). The sole notable exception is the cCbl:UbcH7 complex, which is in fact an inactive E3:E2 pair despite its common use as a primary example of how RING E3s bind E2s. Mutation of R1143 in E4BU ($E4BU^{R1143A}$) generates an E3 unable to shift the population of the UbcH5c-O~Ub conjugate toward closed states, even though consensus E3:E2 interactions remain intact as judged by NMR binding experiments (Fig 4B). Titrations of ^{15}N-labeled UbcH5c with either wild-type E4BU or $E4BU^{R1143A}$ demonstrate that there is little or no significant change in the strength of the E2:E3 binding interaction associated with loss of the hydrogen bond (Fig S5B). Importantly, the hydrogen bond-defective mutants $E4BU^{R1143A}$ or $E4BU^{R1143M}$ show no ability to activate Ub transfer in auto-ubiquitination or oxyester hydrolysis assays (Fig 4C, 2D, S4D). Our results establish that formation of the E3:E2 intermolecular hydrogen bond is required for activation of the E2~Ub conjugate for transfer, even though the contact point is ~15Å from the E2 active site. We propose the hydrogen bond is a key molecular linchpin for initiating the allosteric activation of the E2~Ub conjugate.

Discussion

Previous structural analyses of the assembly of Ub-transfer complexes involving RING/U-box E3 ligases focused primarily on E3:E2 complexes and, more recently, on E2~Ub conjugates in the absence of an E3 (Zheng et al., 2000; Benirschke et al., 2010; Yin et al., 2009; Xu et al., 2008; Deshaies et al., 2009; Zhang et al., 2005; Bentley et al., 2011; Ozkan et al., 2005; Nordquist et al., 2010; Pruneda et al., 2011; Hamilton et al., 2001; Wickliffe et al., 2011; Saha et al., 2011). In general, E2~Ub conjugates exhibit substantial flexibility between the Ub and E2 subunits and display modest to weak interactions with E3s. Thus, binding to an E3 generates a dynamic E3:E2~Ub ensemble that is difficult to define in terms of a single static structure. To structurally characterize such E3:E2~Ub complexes, we employed a variety of NMR-based techniques that 1) directly demonstrate that binding to RING/U-box E3s shifts the ensemble population of E2~Ub conjugates toward more closed, active conformations, 2) expand the “consensus” E3:E2 contact surface required for

E3:E2~Ub assembly, and 3) define critical E3:E2 interactions required for activation of E2~Ub conjugates.

Characterization of UbcH5c~Ub and Ubc13~Ub conjugates by SAXS showed that E2~Ubs sample closed conformations in the absence of an E3, but the E2~Ub closed state is sparsely populated (Pruneda et al., 2011). Despite observations of closed E2~Ub conformations in the absence of an E3, direct evidence regarding the nature of the conjugate within the active E3:E2~Ub complex has been elusive. The NMR and mutational studies presented here demonstrate that binding to RING and U-box E3s increases the population of closed conformations in UbcH5c~Ub and other E2~Ub conjugates. Mutations that selectively disrupt closed conformations (e.g., Ub^{I44A} and $UbcH5c^{L104Q}$) also disrupt Ub transfer activity and E3-enhanced aminolysis (Fig 2) despite our finding that "consensus" E3:E2 binding interactions remain intact (see Fig 1A). Introduction of the L104Q mutation into the structurally analogous position in several other E2s similarly impairs E3-enhanced reactivity of the E2~Ub conjugates. Such mutations not only abrogate the ability of E4BU and BRCA1 to facilitate Ub transfer, but also disrupt Ub-transfer activity catalyzed by other diverse RING E3s (Fig 3B). Thus, we demonstrate that there is a direct link between RING/U-box-facilitated Ub transfer and the induction of an E2~Ub closed conformational state, and that conformational biasing toward closed populations is a feature shared by numerous RING and U-box E3s to activate cognate E2~Ub conjugates for Ub transfer.

How do RING/U-box E3s enhance the population of reactive E2~Ub conjugates? Our studies of the E4BU:UbcH5c~Ub ternary complex identify E4BU R1143 as a key determinant. R1143 is part of a Φ-x-(K/R) motif (F1141, N1142, and R1143 in E4B; L63, C64, and K65 in BRCA1) that is highly conserved among RINGs and U-box E3s. Even the class of bacterial effector E3s that is structurally homologous to eukaryotic U-boxes shows conservation at the analogous position. This is remarkable as bacterial and eukaryotic U-box-type E3s share almost no sequence homology despite having similar structures, suggesting their convergent evolution and highlighting the pivotal role played by the E3 hydrogen bond donor residue in Ub transfer (Fig S2B).

Our NMR studies on wild-type and ligase-inactive mutant proteins allow us to define three discrete requirements for the formation of an active E3:E2~Ub complex and subsequent catalyzed Ub transfer (Fig 5A, wild-type). The first requirement involves formation of the consensus E3:E2 binding interaction as observed in previous crystallographic and NMR studies (Fig 5, dark blue). This interaction is largely conserved among various E3:E2 complexes and can be disrupted with point mutations in the binding interface (e.g. $UbcH5c^{A96D}$ or $BRCA1^{I26A}$; Fig 5B, class "a" mutation). The second requirement for an active E3:E2~Ub complex involves the formation of an intermolecular hydrogen bond from a side chain in the E3 Loop 2 Φ-x-(K/R) motif to a backbone carbonyl at the C-terminal end of the 3_{10} helix in the E2. This interaction does not significantly contribute to the affinity of the E3:E2 complex, but its formation (detected as CSPs in E2 resonances 87–93 within the E2 3_{10} helix) is essential for catalysis. CSPs resulting from the E3:E2 hydrogen bond define an allosteric pathway that links the E3 binding interface to the E2 active site (Fig 5, cyan). Direct experimental evidence shows that the effects of the hydrogen bond extend to the N-terminal end of the 3_{10} helix where a conserved Asp (UbcH5c Asp87) occupies a cleft near the E2 active site. UbcH5c Asp87 is sensitive to steric mutations suggesting it may play a role in controlling access to E2~Ub closed conformations (Wenzel et al., 2011). Consistent with this model, preliminary analysis of the $UbcH5c^{D87E}$-O~Ub conjugate indicates an inability to adopt closed conformations in response to E4BU binding. The allosteric linkage can be broken by mutation of the conserved E3 K/R residue (e.g., E4B R1143A), a mutation that also abrogates formation of closed E2~Ub conformations and the ability to transfer Ub *in vitro* (Fig 5C, class "b" mutation).

The third requirement for an active E3:E2~Ub complex is E3:E2 interactions that allow E2~Ub conjugates to adopt closed conformational states with high frequency. Direct experimental evidence for the closed states comes from the observation of CSPs in the residues surrounding the hydrophobic Ile44 surface of Ub and exposed hydrophobic residues in Helix 2 of the E2 (Fig 5, red). CSPs associated with closed E2~Ub conformations are also observed in E2 active site residues 75, 77, and 86. Point mutations in the E2:Ub interface (e.g. UbcH5c^{L104Q} and Ub^{I44A}) selectively disrupt E3-mediated formation of E2~Ub closed conformations (Fig 5D, class "c" mutations). The three types of interactions are each necessary but none is sufficient on its own. Thus, distinct sets of interactions link E3:E2 binding to increases in the population of closed E2~Ub conformational states and to E3-mediated enhancement of Ub transfer activity. This linkage between E3 binding and the resulting shift toward E2~Ub closed conformations (Fig 5, dark blue – cyan – red) defines a model for the allosteric activation of E2~Ub conjugates by RING and U-box E3s.

The E3:E2~Ub structural model (Fig 1C) suggests additional interactions that could stabilize E2~Ub closed conformations. The N-terminal region of Ub β-strand 2 in some closed states are in proximity to the E3 suggesting a potential E3:Ub contact surface. Such an interaction could enhance the affinity of an E3 for an E2~Ub conjugate over a free E2. Recently, a difference in affinity of nearly 50-fold was reported for binding of the E3 Rbx1 to Cdc34~Ub over free Cdc34 (Spratt et al., 2012). However, binding of free UbcH5c or UbcH5c~Ub to either E4BU or BRCA1 shows remarkably little difference in apparent affinities, as observed in NMR-based competition measurements (Fig S5C). Our model of the E4BU:UbcH5c~Ub complex predicts only few interactions between the C-terminal regions of E4BU Loop 2 and β-strand 2 of Ub. Small CSPs are observed in this region of Ub, but are more consistent with infrequent contacts between E3 and Ub rather than a defined E3:Ub contact surface. The Ub residue that most frequently approaches E4BU is Thr12, but its mutation to Ala or Glu has no impact on observed Ub transfer activity (Fig S4E). Furthermore, the region of RING/U-box E3s that might mediate E3:Ub contacts shows poor sequence conservation outside of the Φ-x-(K/R) motif. Together, these observations argue against the presence of an E3:Ub interaction surface that is broadly shared among the family of RING/U-box E3 ligases.

Our model for assembly and activation of E3:E2~Ub complexes provides a framework for understanding how both post-translational E2~Ub modifications and small molecule ligands may impact Ub transfer activity. UbcH5 contains several acidic residues (Asp42, Asp112, Asp116, and Asp117) that interact with basic residues on Ub (Arg42, Lys48, and Arg72). In other E2s, structurally analogous sites contain serine residues that have been found to be sites of phosphorylation. This suggests that Ub transfer can be regulated by modulating the negative electrostatic potential in regions of the E2:Ub interface which, in turn, alter the ability of E2~Ub conjugates to adopt closed conformations. For example, positions that correspond structurally to UbcH5c Asp112 are conserved as either Asp or Ser in a large number of E2s. Yeast E2 Ubc1 Ser115 is a site of reversible phosphorylation associated with a phenotype in which yeast display enhanced tolerance to environmental stresses (Meena et al., 2011). Our E4BU:UbcH5c~Ub model predicts that the phosphorylation of Ubc1 Ser115 would enhance the E2:Ub electrostatic interaction, thereby promoting the activation of Ub transfer. Another example involves the bacterial effector protein CHBP which catalyzes deamidation of Ub Gln40 to yield Glu (Cui et al., 2010). The Ub Q40E modification would create an unfavorable electrostatic contact in the closed E2:Ub interface and, in fact, Ub modified at this position is not active in ubiquitination reactions (Cui et al., 2010). A third example is the highly specific inhibitor of the E2 Cdc34 found in a high-throughput small molecule screen, which blocks E3-mediated Ub transfer without affecting assembly of the ubiquitination machinery (Ceccarelli et al., 2011). A Cdc34/inhibitor co-crystal structure revealed that the inhibitor binds Cdc34 directly above Helix 2 causing a 2Å shift in Helix 2

and active site residues relative to the unliganded E2. Our structural analysis of the RING/U-box E3:E2~Ub complex suggests that such a structural perturbation may block adoption of a Cdc34~Ub closed conformation and E3-mediated Ub transfer by preventing Ub:Cdc34 interactions in the closed state.

RING/U-box E3s have traditionally been thought to function by simultaneously binding both substrate and E2~Ub conjugate to facilitate Ub transfer. The results presented here define an additional essential role for RING/U-box E3 ligases in promoting ubiquitin transfer. Assembly of a RING/U-box E3:E2~Ub ligase complex biases the E2~Ub conjugate toward closed conformational states that are more reactive toward lysine. The linchpin of the E2~Ub activation is formation of a conserved E3:E2 intermolecular hydrogen bond that allows for E2~Ub allosteric activation, not by stabilizing a discrete protein conformation, but by shifting the E2~Ub conformational ensemble toward more reactive states. The ability to form a closed E2~Ub complex is essential to the function of a diverse array of both E2s and RING/U-box E3s, illuminating a general strategy that can be exploited by other RING/U-box family members. The molecular basis for allosteric activation of E2~Ub conjugates presented here provides new insights into how RING/U-box E3s function and offers valuable tools for investigation of the biological function of the largest class of E3 Ub-ligases.

Experimental Procedures

Plasmids, protein expression and purification

Plasmid constructs, expression, and purification of E1, Ub, UbcH5c, BRCA1$^{1–112}$/BARD1$^{26–140}$, BRCA1$^{1–304}$/BARD1$^{26–327}$, Ube2k, Ube2n, Ube2e1, E4BU, E4BU^{+20}, E6AP, and HHARI were previously described (Christensen et al., 2007; Brzovic et al., 2003; Nordquist et al., 2010; Huang et al., 1999; Wenzel et al., 2011). SspH1 was produced and purified as described for SspH2 (Levin et al., 2010). Point mutations were produced via Quikchange site-directed mutagenesis (Stratagene) and confirmed by DNA sequencing. All proteins were expressed in BL21 *Escherichia coli* (Invitrogen) in either rich LB media or isotope supplemented minimal MOPS media (Cambridge Isotopes). Proteins were stored in 25 mM sodium phosphate 150 mM NaCl (pH 7.0) at either 4°C or −80°C.

NMR Spectroscopy – Chemical Shift Perturbation and Paramagnetic Relaxation Enhancement

NMR spectra were recorded on either a 500 MHz Bruker Avance II (University of Washington) or a 750 MHz Varian INOVA spectrometer (Pacific Northwest National Laboratories, Richland, WA). UbcH5c-O~Ub was prepared as previously described using the structurally analogous active site Cys-to-Ser mutation in UbcH5c to improve conjugate stability, and the S22R mutation to prevent noncovalent Ub binding on the “backside” of UbcH5c (Brzovic et al., 2006). Spectra were recorded at 25°C in 25 mM sodium phosphate 150 mM NaCl (pH 7.0) 10% D_2O. All titration datasets were collected using $^{1}H,^{15}N$-HSQC-TROSY experiments with 220 μM labeled protein with or without addition of unlabeled partners. Data were processed using NMRPipe/NMRDraw (Delaglio et al., 1994), and visualized with NMRView (Johnson et al., 1994). Chemical shift perturbations were calculated with the formula $\Delta\delta_j = [(\Delta\delta_j{}^{15}N/5)^2 + (\Delta\delta_j{}^{1}H)^2]^{1/2}$. Ub-K11C, covalently modified with 4-(2-iodoacetamido)-TEMPO (Sigma-Aldrich) as previously described (Pruneda et al., 2011), was conjugated to UbcH5c, and the conjugate was purified by gel filtration. Active and ascorbate-reduced spectra were recorded in the presence of >1 molar equivalent E4BU, and resonances with an I/I_{red} ratio lower than 1.5 standard deviation from the mean were deemed significantly affected by the probe.

NMR Spectroscopy- Relaxation Analysis

Heteronuclear R1 and NOE parameters were measured using standard protocols (Palmer, 2004). NMR spectra were recorded on 600 and 900 MHz Bruker Avance III spectrometers (Vanderbilt University). ^{15}N-UbcH5c-O~^{15}N-Ub and E4BU were prepared as described above and data were collected at 20°C in 30 mM sodium citrate (pH 5.75), 150 mM NaCl, 8% D_2O. Samples contained 200 μM labeled UbcH5c-O~Ub with or without 600 μM unlabeled E4BU. The conjugate slowly hydrolyzes when bound to E4BU, so multiple samples were used for the ternary complex. These samples were prepared just before use from concentrated stocks and were limited to 1.5 days of data collection. Attempts to acquire ^{15}N-R2 experiments for the ternary complex were stymied by the limited hydrolysis of conjugate, since the signals from free Ub dominated the spectrum. We therefore resorted to measuring R1 and NOE at multiple fields. The recovery delays for ^{15}N-R1 experiments were 7.5 s and 12 s (600 and 900 MHz, respectively), and a three second saturation period was used for the {^{1}H}-^{15}N NOE. Time delays for the R1 measurements were 0.1, 0.4, 0.8, 1.2, 1.8, 2.5, and 4 s at 600 MHz, and 0.1, 0.4, 0.8, 1.2, 2, 3, and 5 s at 900 MHz. The data were processed in Topspin (Bruker) and analyzed in Sparky (Goddard, UCSF). The NOE was calculated as the ratio of intensities I_{sat}/I_{ref}, and the NOE error was calculated such that $(\text{NOE err/NOE})^2 = [(I_{ref}\ \text{err}/I_{ref})^2 + (I_{sat}\ \text{err}/I_{sat})^2]$ and the error of each intensity measurement is the rmsd noise of each plane. Residues with NOE < 0.7 or having fewer than 3 of the 4 points determined were removed from analysis. The remaining Ub residues (48 for UbcH5c-O~Ub sample and 51 for ternary complex with E4BU) were each fit to a local isotropic correlation time (τiso) using relax (d'Auvergne et al., 2008). These values were then input into the quadric_diffusion program (AG Palmer, based on Lee et al., 1997) to fit global diffusion tensors when using a structural model of Ub oriented to the inertial mass tensor. Among the isotropic, axial, and anisotropic models, the best statistical fit was obtained using axial symmetric diffusion tensors. Models of the diffusion tensors were created with relax and visualized using PYMOL.

Computational Modeling

Docking experiments were performed using HADDOCK 2.124. Previous studies have shown that the E4BU, UbcH5c, and Ub subunits do not undergo detectable conformational changes when interacting with their protein partners (Benirschke et al., 2010; Pruneda et al., 2011). Therefore, available NMR and X-ray crystallographic structures of the individual protein components were used as input. Input structures for UbcH5c, Ub, and E4BU were taken from solution NMR ensembles of Protein Data Bank entries 2FUH (chain A), 1XQQ, and 2KR4, respectively. Unambiguous distance and dihedral restraints were used to model conjugation of the Ub C-terminus to the UbcH5c active site cysteine, and Ub residues 72–76 were allowed full flexibility. Definition of active and passive residues for ambiguous restraints was based on chemical shift perturbation data and was filtered for solvent accessibility. Ambiguous interaction restraints are listed in Table S1.

Small nucleophile reactivity assays

Reactivity assays involving Ub transfer to free lysine were performed as previously described (Wenzel et al., 2011). Briefly, an E2~HA-Ub(K0) conjugate is formed (this ubiquitin construct contains arginine or methionine mutations at all lysine positions to prevent Ub chain formation). The conjugate is then combined with BC_{112}/BD_{140} and free lysine. Reaction samples are quenched in non-reducing SDS load buffer. Ub transfer to lysine is monitored by disappearance of the E2~Ub species, as observed by western blot probing for the HA epitope on Ub.

Hydrolysis of the UbcH5c-O~Ub conjugate was monitored by ^{1}H-NMR spectra recorded in 25 mM sodium phosphate 150 mM NaCl (pH 7.0) 10% D_2O at 25°C. 220 μM UbcH5c-

O~Ub was combined (when applicable) with a 1:1 molar equivalency of E4BU. Spectra were processed and analyzed using MestReNova (Mestrelab Research). The integral of a 0.2 ppm window spanning the conjugated-Asn77 backbone amide resonance was calculated for each spectrum; baseline correction within each spectrum was performed by subtraction of the integral from a 0.2 ppm window in a neighboring region with no observable resonances.

E3 auto-ubiquitination reactions

Auto-ubiquitination reactions with BC_{304}/BD_{327} and $E4BU^{+20}$ were performed as previously described (Wenzel et al., 2011; Christensen et al., 2007; Nordquist et al., 2010). Reactions including $RNF8^{239–485}$, $MDM2^{FL}$, $E6AP^{494–875}$, $SspH1^{FL}$, and $HHARI^{177–395}$ were performed similarly to those with BC_{304}/BD_{327}. Briefly, a mixture of E1, E2, E3, and Ub is incubated with $ATP/MgCl_2$ to initiate the reaction. Samples are quenched by boiling in SDS loading buffer and ubiquitination products are visualized either by Coomassie staining or western blotting for FLAG-BRCA1 or HA-Ub components.

Supplementary Material

Refer to Web version on PubMed Central for supplementary material.

Acknowledgments

We thank V. Vittal, K. Dove, N. Zheng, A.G. Palmer, and W. Hol for discussions and critical reading of the manuscript. We acknowledge B. Larimore for performing the experiment shown in Supplemental Figure 7C in the N. Zheng and B. Clurman laboratories. A portion of this research was performed using EMSL, a national user facility sponsored by the Department of Energy's Office of Biological and Environmental Research and located at PNNL. This work was supported by National Institutes of Health Grants R01 GM088055 (R.E.K.) and R01 GM075156 (W.J.C.), and the U.S. Public Health Service Grant NRSA 2T32 GM007270 from the National Institute of General Medical Sciences (J.N.P.). Access to instrumentation was supported by grants P30 ES0000267 (Vanderbilt University Center in Molecular Toxicology) and P50 CA068485 (Vanderbilt-Ingram Cancer Center) from the National Institutes of Health.

References

1. Song J, Wang J, Jozwiak AA, Hu W, Swiderski PM, Chen Y. Stability of thioester intermediates in ubiquitin-like modifications. Protein Sci. 2009; 18:2492–2499. [PubMed: 19785004]
2. Wenzel DM, Lissounov A, Brzovic PS, Klevit RE. UBCH7 reactivity profile reveals parkin and HHARI to be RING/HECT hybrids. Nature. 2011; 474:105–108. [PubMed: 21532592]
3. Zheng N, Wang P, Jeffrey PD, Pavletich NP. Structure of a c-Cbl-UbcH7 complex: RING domain function in ubiquitin-protein ligases. Cell. 2000; 102:533–539. [PubMed: 10966114]
4. Benirschke RC, Thompson JR, Nomine Y, Wasielewski E, Juranic N, Macura S, Hatakeyama S, Nakayama KI, Botuyan MV, Mer G. Molecular Basis for the Association of Human E4B U Box Ubiquitin Ligase with E2-Conjugating Enzymes UbcH5c and Ubc4. Structure. 2010; 18:955–965. [PubMed: 20696396]
5. Yin Q, Lin SC, Lamothe B, Lu M, Lo YC, Hura G, Zheng L, Rich RL, Campos AD, Myszka DG, et al. E2 interaction and dimerization in the crystal structure of TRAF6. Nat Struct Mol Biol. 2009; 16:658–666. [PubMed: 19465916]
6. Xu Z, Kohli E, Devlin KI, Bold M, Nix JC, Misra S. Interactions between the quality control ubiquitin ligase CHIP and ubiquitin conjugating enzymes. BMC Struct Biol. 2008; 8:26. [PubMed: 18485199]
7. Deshaies RJ, Joazeiro CA. RING domain E3 ubiquitin ligases. Annu Rev Biochem. 2009; 78:399–434. [PubMed: 19489725]
8. Zhang M, Windheim M, Roe SM, Peggie M, Cohen P, Prodromou C, Pearl LH. Chaperoned ubiquitylation - crystal structures of the CHIP U-box E3 ubiquitin ligase and a CHIP-Ubc13-Uev1a complex. Mol Cell. 2005; 20:525–538. [PubMed: 16307917]

9. Bentley ML, Corn JE, Dong KC, Phung Q, Cheung TK, Cochran AG. Recognition of UbcH5c and the nucleosome by the Bmi1/Ring1b ubiquitin ligase complex. EMBO J. 2011; 30:3285–3297. [PubMed: 21772249]
10. Ozkan E, Yu H, Deisenhofer J. Mechanistic insight into the allosteric activation of a ubiquitin-conjugating enzyme by RING-type ubiquitin ligases. PNAS. 2005; 102:18890–18895. [PubMed: 16365295]
11. Welcsh PL, Owens KN, King MC. Insights into the functions of BRCA1 and BRCA2. Trends Genet. 2000; 16:69–74. [PubMed: 10652533]
12. Welcsh PL, King MC. BRCA1 and BRCA2 and the genetics of breast and ovarian cancer. Hum Mol Genet. 2001; 10:705–13. [PubMed: 11257103]
13. Yu V. Caretaker Brca1: keeping the genome in the straight and narrow. Breast Cancer Res. 2000; 2:82–85. [PubMed: 11250695]
14. Scully R, Puget N. BRCA1 and BRCA2 in hereditary breast cancer. Biochimie. 2002; 84:95–102. [PubMed: 11900881]
15. Cyr DM, Höhfeld J, Patterson C. Protein quality control: U-box-containing E3 ubiquitin ligases join the fold. Trends Biochem Sci. 2002; 27:368–375. [PubMed: 12114026]
16. Richly H, Rape M, Braun S, Rumpf S, Hoege C, Jentsch S. A series of ubiquitin binding factors connects CDC48/p97 to substrate multiubiquitylation and proteasomal targeting. Cell. 2005; 120:73–84. [PubMed: 15652483]
17. Brzovic PS, Keeffe JR, Nishikawa H, Miyamoto K, Fox D, Fukuda M, Ohta T, Klevit RE. Binding and recognition in the assembly of an active BRCA1/BARD1 ubiquitin-ligase complex. PNAS. 2003; 100:5646–5651. [PubMed: 12732733]
18. Christensen DE, Brzovic PS, Klevit RE. E2-BRCA1 RING interactions dictate synthesis of mono- or specific polyubiquitin chain linkages. Nat Struct Mol Biol. 2007; 14:941–948. [PubMed: 17873885]
19. Nordquist KA, Dimitrova YN, Brzovic PS, Ridenour WB, Munro KA, Soss SE, Caprioli RM, Klevit RE, Chazin WJ. Structural and functional characterization of the monomeric U-box domain from E4B. Biochemistry. 2010; 49:347–355. [PubMed: 20017557]
20. Pruneda JN, Stoll KE, Bolton LJ, Brzovic PS, Klevit RE. Ubiquitin in Motion: Structural studies of the E2~Ub conjugate. Biochemistry. 2011; 50:1624–1633. [PubMed: 21226485]
21. Hamilton KS, Ellison MJ, Barber KR, Williams RS, Huzil JT, McKenna S, Ptak C, Glover M, Shaw GS. Structure of a conjugating enzyme-ubiquitin thiolester intermediate reveals a novel role for the ubiquitin tail. Structure. 2001; 9:897–904. [PubMed: 11591345]
22. Wickliffe KE, Lorenz S, Wemmer DE, Kuriyan J, Rape M. The mechanism of linkage-specific ubiquitin chain elongation by a single-subunit E2. Cell. 2011; 144:769–781. [PubMed: 21376237]
23. Saha A, Lewis S, Kleiger G, Kuhlman B, Deshaies RJ. Essential role for ubiquitin-ubiquitin-conjugating enzyme interaction in ubiquitin discharge from cdc34 to substrate. Mol Cell. 2011; 42:75–83. [PubMed: 21474069]
24. Brzovic PS, Lissounov A, Christensen DE, Hoyt DW, Klevit RE. A UbcH5c/Ubiquitin noncovalent complex is required for processive BRCA1-directed ubiquitination. Mol Cell. 2006; 21:873–880. [PubMed: 16543155]
25. de Vries SJ, van Dijk M, Bonvin AM. The HADDOCK web server for data-driven biomolecular docking. Nat Protoc. 2010; 5:883–897. [PubMed: 20431534]
26. Palmer AG. NMR Characterization of the dynamics of biomacromolecules. Chem Rev. 2004; 104:3623–3640. [PubMed: 15303831]
27. Spratt DE, Wu K, Kovacev J, Pan ZQ, Shaw GS. Selective recruitment of an E2~ubiquitin complex by an E3 ubiquitin ligase. J Biol Chem. 2012 Epub ahead of print. 10.1074/jbc.M112.353748
28. Meena RC, Thakur S, Nath S, Chakrabarti A. Tolerance to thermal and reductive stress in Saccharomyces cerevisiae is amenable to regulation by phosphorylation-dephosphorylation of ubiquitin conjugating enzyme (Ubc1) S97 and S115. Yeast. 2011; 28:783–793. [PubMed: 21996927]

29. Cui J, Yao Q, Li S, Ding X, Lu Q, Mao H, Liu L, Zheng N, Chen S, Shao F. Glutamine deamidation and dysfunction of ubiquitin/NEDD8 induced by a bacterial effector family. Science. 2010; 329:1215–1218. [PubMed: 20688984]

30. Ceccarelli DF, Tang X, Pelletier B, Orlicky S, Xie W, Plantevin V, Neculai D, Chou YC, Ogunjimi A, Al-Hakim A, et al. An allosteric inhibitor of the human Cdc34 ubiquitin-conjugating enzyme. Cell. 2011; 145:1075–1087. [PubMed: 21683433]

31. Huang L, Kinnucan E, Wang G, Beaudenon S, Howley PM, Huibregtse JM, Pavletich NP. Structure of an E6AP-UbcH7 Complex: Insights into Ubiquitination by the E2-E3 Enzyme Cascade. Science. 1999; 286:1321–1326. [PubMed: 10558980]

32. Levin I, Eakin C, Blanc MP, Klevit RE, Miller SI, Brzovic PS. Identification of an unconventional E3 binding surface on the UbcH5~Ub conjugate recognized by a pathogenic bacterial E3 ligase. PNAS. 2010; 107:2848–2853. [PubMed: 20133640]

33. Delaglio F, Grzesiek S, Vuister GW, Zhu G, Pfeifer J, Bax A. NMRPipe: A multidimensional spectral processing system based on UNIX pipes. J Biomol NMR. 1994; 6:277–293. [PubMed: 8520220]

34. Johnson BA, Blevins RA. NMRView: a computer program for the visualization and analysis of NMR data. J Biomol NMR. 1994; 4:603–614. [PubMed: 22911360]

35. Goddard, TD.; Kneller, DG. SPARKY. Vol. 3. University of California; San Francisco:

36. d'Auvergne EJ, Gooley PR. Optimisation of NMR dynamic models I. Minimisation algorithms and their performance within the model-free and Brownian rotational diffusion spaces. J Biomol NMR. 2008; 40:107–119. [PubMed: 18085410]

37. Lee LK, Rance M, Chazin WJ, Palmer AG. Rotational diffusion anisotropy of proteins from simultaneous analysis of 15N and 13Calpha nuclear spin relaxation. J Biomol NMR. 1997; 9:287–298. [PubMed: 9204557]

Highlights

- Binding to RING/U-box E3s shifts UbcH5c~Ub towards closed conformations
- Closed conformations are linked to E3 enhancement of E2~Ub reactivity
- Induction of closed E2~Ub conformations is a general mechanism of RING/U-box E3s
- A conserved E3:E2 hydrogen bond is required for allosteric activation of Ub transfer

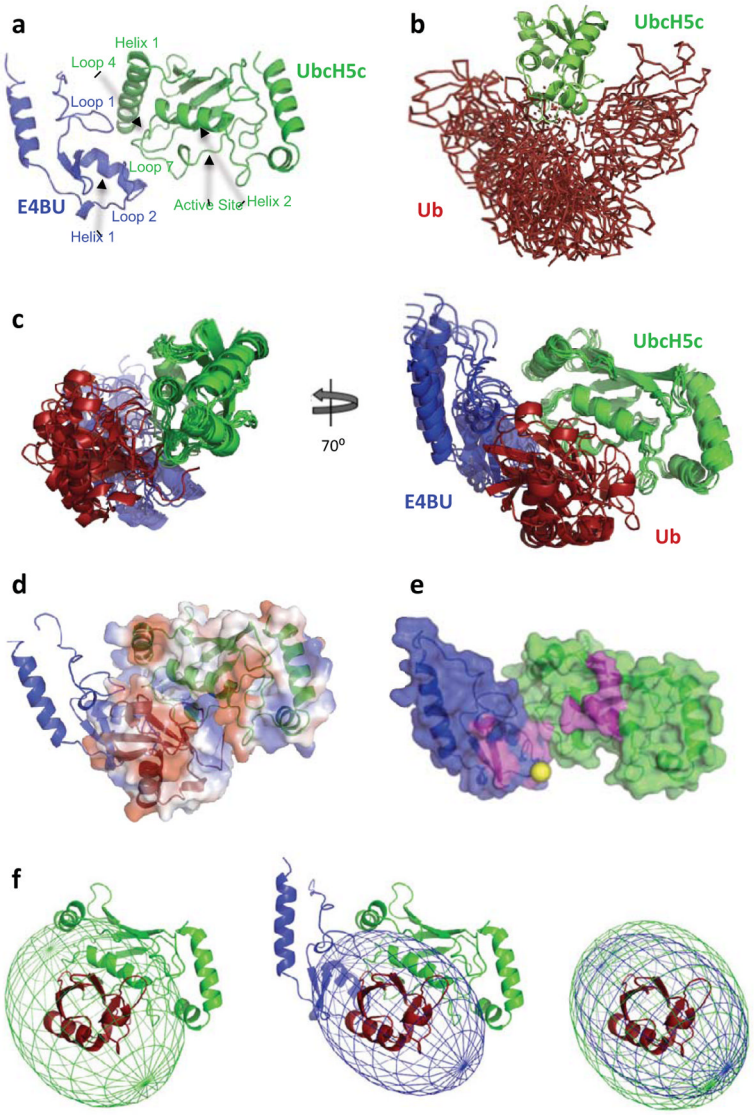

Figure 1. Model of the E4BU:UbcH5c~Ub complex

a) The E4BU:UbcH5 complex (PDB ID 3L1Z) is shown as a representative structure of RING/U-box E3:E2 structures. Structural features relevant to this work are noted. **b)** A side-on view of the UbcH5c~Ub structural ensemble generated from small angle X-ray data (Pruneda et al., 2011). **c)** Five representative structures of the top-scored HADDOCK cluster, aligned on UbcH5c (green); E4BU and Ub are shown in blue and red, respectively. For comparison, the view on the left is comparable to that shown in panel b). **d)** An electrostatic surface is shown for a representative E4BU:UbcH5c~Ub structure within the top-scored HADDOCK cluster. Note the expansive interaction between an acidic patch on UbcH5c and a basic region on Ub. **e)** Regions affected by the spin-labeled conjugate (i.e., Ub-K11SL) are painted in magenta (> 1.5 sd from the mean I_{act}/I_{red}); the alpha carbon of Ub residue 11 from one member of the ensemble is shown as a yellow sphere for reference. **f)** Mesh representation of the axially symmetric rotational diffusion tensors for Ub from the UbcH5c-O~Ub conjugate (left, green) and the ternary complex with E4BU (middle, blue), and aligned and superimposed (right).

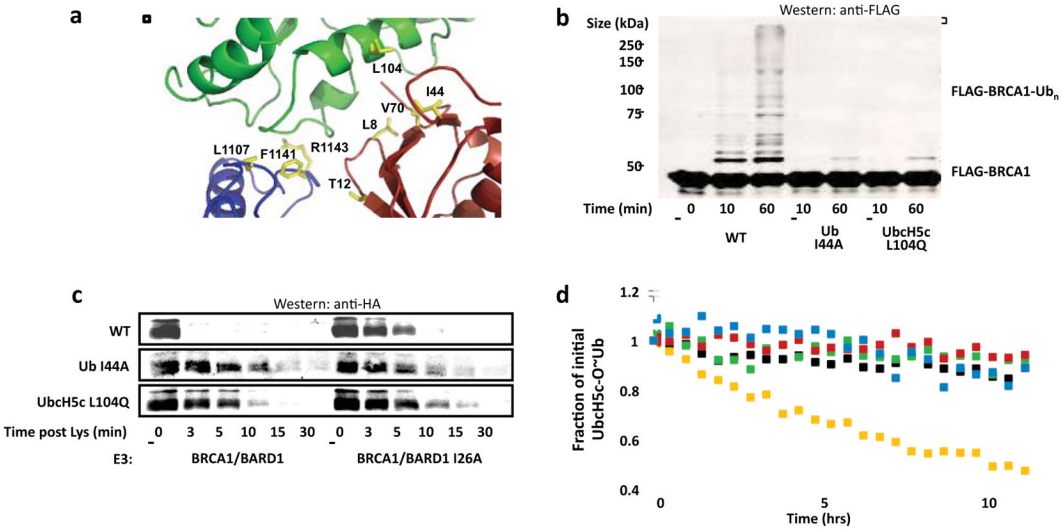

Figure 2. Mutations that disable RING/U-box E3-mediated UbcH5c~Ub conformational change disrupt activity

a) Close-up of protein-protein interactions within the ternary complex model. Residues chosen for mutation (yellow sticks) include E4BU F1141 and R1143, UbcH5c L104, and Ub L8, I44, V70, and T12. E4BU L1107 (mutation to Ala disrupts E3:E2 interaction) is shown for reference. **b)** Auto-ubiquitination activity assays with BC_{304}/BD_{327} and UbcH5c, as monitored by Western analysis following FLAG-BRCA1. Reaction components are WT except when indicated. c) Lysine reactivity assays with BC_{112}/BD_{140} and UbcH5c. Reaction components are WT except when indicated. Western blot for HA-Ub(K0) to monitor decay of the UbcH5c~HA-Ub(K0) conjugate is shown. Two reaction time courses are shown for each E2~Ub: on the left, time course in the presence of WT BRCA1/BARD1 (specify the construct) and on the right, time course in the presence of I26A-BRCA1/BARD1, which does not bind to UbcH5 (Brzovic et al., 2003). **d)** Time course of the hydrolysis of UbcH5c oxyesters in the presence and absence of E4BU, as followed by 1-D NMR. The y-axis shows the fraction of oxy-ester remaining, as measured by integration of the UbcH5c Asn77 resonance at its conjugated position. Curves for UbcH5c-O~Ub and E4BU:UbcH5c-O~Ub samples are presented in black and yellow, respectively. Replacement of WT components in the E4BU:UbcH5c-O~Ub complex with Ub^{I44A}, $UbcH5c^{L104Q}$, or $E4BU^{R1143A}$ are colored in red, green, and blue, respectively.

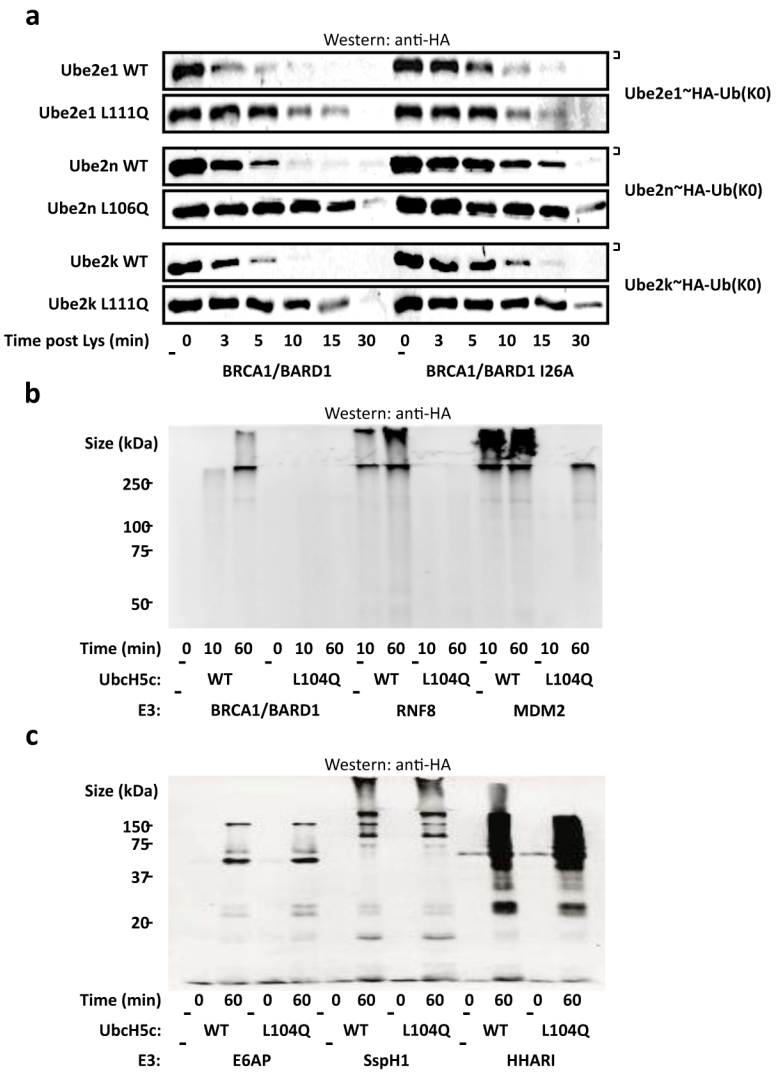

Figure 3. Conformational activation of the E2~Ub conjugate is required for RING/U-box E3 activity

a) Lysine reactivity assays for Ube2e1, Ube2n, and Ube2k with BC_{112}/BD_{140}. E2 identity is listed in column at left. Western blot for HA-Ub(K0) to follow decay of the E2~HA-Ub(K0) conjugate is shown. **b)** Auto-ubiquitination assays of RING/U-box E3s with $UbcH5c^{WT}$ and $UbcH5c^{L104Q}$. Western blot following HA-Ub is shown. **c)** As in b), but with HECT-type E3s, as indicated.

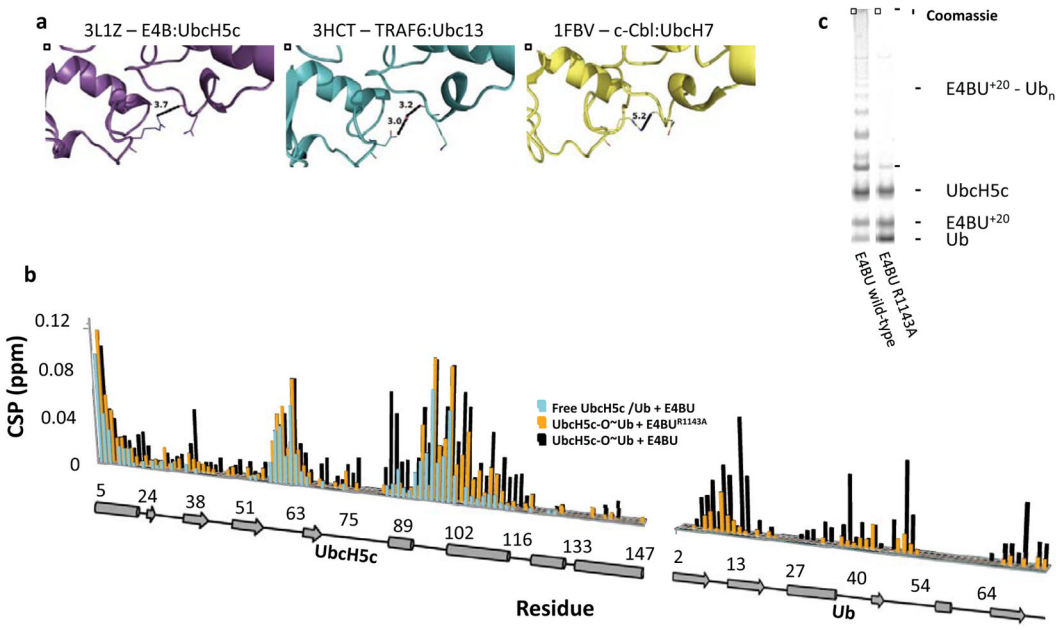

Figure 4. A conserved E3:E2 hydrogen bond is required for E3-mediated Ub transfer

a) Examples of RING/U-box E3:E2 interactions observed in deposited crystal structures include E4B:UbcH5c (3L1Z, left), TRAF6:Ubc13 (3HCT, center), and c-Cbl:UbcH7 (1FBV, right). 3L1Z represents the common case in which a conserved E3 basic residue directly hydrogen bonds the E2 backbone. TRAF6, which lacks the conserved basic residue, maintains this interaction through an ordered water molecule. In contrast, no hydrogen bond is observed in the c-Cbl:UbcH7 complex, which is in fact an inactive pair. **b)** Addition of 0.5 molar eq. of $E4BU^{R1143A}$ to ^{15}N-UbcH5c-O~^{15}N-Ub (orange) results in CSPs plotted in the histogram. 0.5 molar eq. titration points of $E4BU^{WT}$ into free ^{15}N-UbcH5c/Ub (cyan) and ^{15}N-UbcH5c-O~^{15}N-Ub (black) are shown for reference. **c)** $E4BU^{+20}$ auto-ubiquitination assays show that the $E4B^{R1143A}$ mutant is deficient in Ub transfer activity. Gel slices taken from figure S4B.

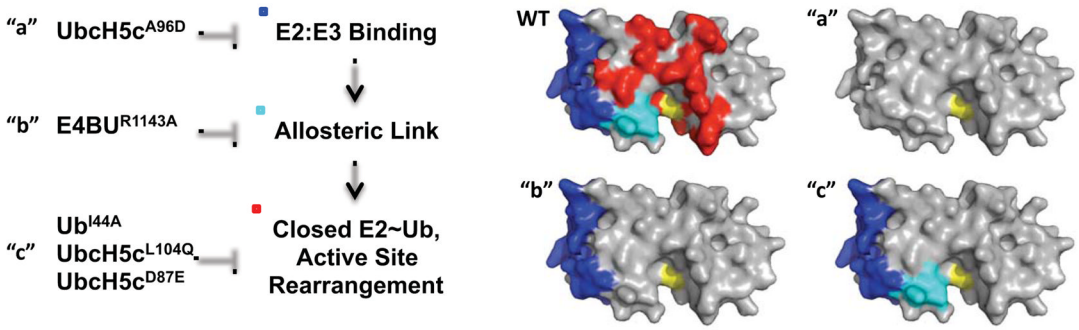

Figure 5. Allosteric activation by RING/U-Box E3s involves three discrete structural requirements

Formation of an active E3:E2~Ub complex depends on three structural requirements: 1) A consensus E3:E2 interaction at E2 Helix 1, Loop 4, and Loop 7 (reported by CSPs highlighted in dark blue), 2) Formation of an intermolecular E3:E2 hydrogen bond that causes secondary effects permeating through the E2 3_{10} helix (reported by CSPs highlighted in cyan), and 3) Overpopulation of closed E2~Ub conformations that result in additional changes surrounding the active site (reported by CSPs highlighted in red). Each requirement can be targeted with specific point mutations. Class "a" mutations such as UbcH5c Loop 7 A96D disrupt formation of the consensus E3:E2 interaction. The essential intermolecular hydrogen bond can be disrupted via a class "b" mutation such as E4B R1143A. Finally, formation of closed E2~Ub conformations can be blocked with class "c" mutations such as UbcH5c D87E, UbcH5c L104Q, or Ub I44A.